Brg1 governs distinct pathways to direct multiple aspects of mammalian neural crest cell development

Wei Li[a,1], Yiqin Xiong[a,1], Ching Shang[a], Karen Y. Twu[a], Calvin T. Hang[a], Jin Yang[a], Pei Han[a], Chieh-Yu Lin[a], Chien-Jung Lin[a], Feng-Chiao Tsai[b], Kryn Stankunas[a], Tobias Meyer[b], Daniel Bernstein[c], Minggui Pan[a], and Ching-Pin Chang[a,2]

[a]Division of Cardiovascular Medicine, Department of Medicine, [b]Department of Chemical and Systems Biology, and [c]Division of Pediatric Cardiology, Department of Pediatrics, Stanford University School of Medicine, Stanford, CA 94305

Edited by Eric N. Olson, University of Texas Southwestern Medical Center, Dallas, TX, and approved December 12, 2012 (received for review October 18, 2012)

Development of the cerebral vessels, pharyngeal arch arteries (PAAs). and cardiac outflow tract (OFT) requires multipotent neural crest cells (NCCs) that migrate from the neural tube to target tissue destinations. Little is known about how mammalian NCC development is orchestrated by gene programming at the chromatin level, however. Here we show that Brahma-related gene 1 (Brg1), an ATPase subunit of the Brg1/Brahma-associated factor (BAF) chromatin-remodeling complex, is required in NCCs to direct cardiovascular development. Mouse embryos lacking *Brg1* in NCCs display immature cerebral vessels, aberrant PAA patterning, and shortened OFT. Brg1 suppresses an apoptosis factor, *Apoptosis signal-regulating kinase 1 (Ask1),* and a cell cycle inhibitor, $p21^{cip1}$, to inhibit apoptosis and promote proliferation of NCCs, thereby maintaining a multipotent cell reservoir at the neural crest. Brg1 also supports *Myosin heavy chain 11 (Myh11)* expression to allow NCCs to develop into mature vascular smooth muscle cells of cerebral vessels. Within NCCs, Brg1 partners with chromatin remodeler Chromodomain-helicase-DNA-binding protein 7 (Chd7) on the *PlexinA2* promoter to activate *PlexinA2,* which encodes a receptor for semaphorin to guide NCCs into the OFT. Our findings reveal an important role for Brg1 and its downstream pathways in the survival, differentiation, and migration of the multipotent NCCs critical for mammalian cardiovascular development.

Neural crest cells (NCCs) originate from the neural crest of the dorsal neural tube and migrate to many regions of the embryo, where they differentiate into a variety of local cells, including cardiovascular tissues (1). NCCs that emigrate from the neural crest of rhombomere 6–8 to pharyngeal arches and the heart are essential for the patterning of pharyngeal arch arteries (PAAs) and the cardiac outflow tract (OFT) (2, 3). These NCCs also differentiate into vascular smooth muscle cells (SMCs) of PAAs and the muscular septum of the aorta and pulmonary trunk (4, 5). In contrast, NCCs from the cephalic neural tube migrate to the face and forebrain to form craniofacial bones, as well as SMCs of facial and forebrain vessels (6). Thus, NCCs are critical for the formation of cardiac OFT and vascular supplies of large areas of the body.

Disruption of NCC development, either directly or indirectly, results in many forms of human birth defects with cardiovascular malformations, including Alagille, Carpenter, Ivemark, Leopard, Williams, DiGeorge, and CHARGE syndromes (7). These syndromes involve defects in PAAs or cardiac OFT, such as coarctation of the aorta, interrupted aortic arch, pulmonary artery stenosis, double-outlet right ventricle, tetralogy of Fallot, or persistent truncus arteriosus. During PAA and OFT development, NCCs are regulated by numerous transcription factors, including Pax3, Pbx1/2/3, Tbx1/2/3/20, Msx1/2, Hand2, AP-2a, Cited2, Pitx2, Sox4, Foxc1/c2/d3/h1, Fog2, Gata3/4/6, and Notch/NICD (8). Such extensive involvement of transcription factors indicates the importance of gene programming in NCC, PAA, and OFT development.

DNA is tightly packed by chromatin, and the access of transcription factors to genomic loci depends on the chromatin structure. Chromatin thus acts as a major controller of gene expression. Chromatin structure can be altered by covalent histone modifications through histone-modifying enzymes or by changes in nucleosome position and composition through ATP-dependent chromatin-remodeling factors. Despite the importance of chromatin regulation and NCC-related human diseases, little is known about how NCCs are programmed at the chromatin level for cardiovascular development (8–10). Our studies demonstrate a cell-autonomous function of a chromatin remodeler, Brg1, in NCCs and downstream pathways to orchestrate NCC development in mice.

Brahma-related gene 1 (Brg1) is an essential ATPase subunit of the Swi/Snf-like BAF chromatin-remodeling complex in vertebrates (11). Brg1 hydrolyzes ATP to drive the chromatin remodeling activity of the BAF complex. A recent study indirectly linked Polybromo-BAF (PBAF) (containing Brg1) to the pathogenesis of CHARGE syndrome (12), characterized by coloboma, heart defects, atresia choanae, retarded growth and development, genital hypoplasia, and ear abnormalities/deafness. CHARGE syndrome is caused by haploinsufficiency of a chromodomain chromatin-remodeling factor, *Chromodomain-Helicase-DNA-binding protein 7 (CHD7)* (13), and includes cardiovascular defects in PAA and OFT (14). Although Chd7 knockdown in frog embryos causes abnormal OFT positioning, and Chd7 associates with PBAF in frog embryos (12), there is no direct evidence of the need for Brg1 in NCCs for PAA and OFT development in frogs or mice.

Through tissue-specific deletion of *Brg1* in NCCs, our studies demonstrate a cell-autonomous role of Brg1 in NCCs for the development of cerebral vessels, PAAs, and cardiac OFT in mice. In addition, we identified molecular pathways downstream of Brg1 that control cell apoptosis, proliferation, differentiation, and migration of NCCs.

Results

Deletion of *Brg1* in NCCs Results in Embryonic Lethality. To test Brg1 function in NCCs, we deleted *Brg1* by crossing mice carrying a loxP-flanked allele of *Brg1 ($Brg1^{f}$)* (15) with mice harboring *Wnt1Cre*, whose Cre is active in NCCs (4, 16). To confirm *Brg1* deletion in NCCs, we immunostained Brg1 of embryonic day (E) 10 *Wnt1Cre;$Brg1^{f/f}$* embryos and found that Brg1 proteins were absent in NCCs and NCC-derived tissues, including dorsal root

Author contributions: W.L., Y.X., and C.-P.C. designed research; W.L., Y.X., C.S., K.Y.T., C.T.H., J.Y., P.H., C.-Y.L., C.-J.L., F.-C.T., and K.S. performed research; J.Y., P.H., F.-C.T., and T.M. contributed new reagents/analytic tools; W.L., Y.X., T.M., D.B., M.P., and C.-P.C. analyzed data; and W.L., Y.X., D.B., M.P., and C.-P.C. wrote the paper.

The authors declare no conflict of interest.

This article is a PNAS Direct Submission.

[1]W.L. and Y.X. contributed equally to this work.

[2]To whom correspondence should be addressed. E-mail: chingpin@stanford.edu.

This article contains supporting information online at www.pnas.org/lookup/suppl/doi:10.1073/pnas.1218072110/-/DCSupplemental.

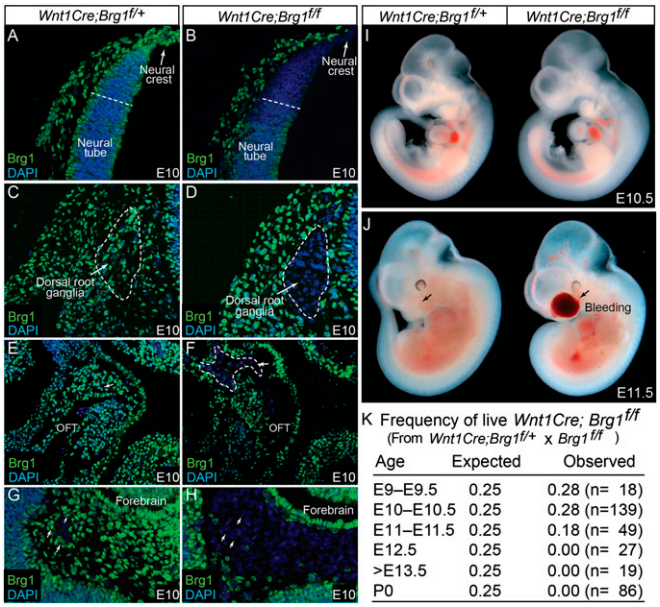

K Frequency of live *Wnt1Cre; Brg1$^{f/f}$* (From *Wnt1Cre;Brg1$^{f/+}$* x *Brg1$^{f/f}$*)

Age	Expected	Observed
E9–E9.5	0.25	0.28 (n= 18)
E10–E10.5	0.25	0.28 (n=139)
E11–E11.5	0.25	0.18 (n= 49)
E12.5	0.25	0.00 (n= 27)
>E13.5	0.25	0.00 (n= 19)
P0	0.25	0.00 (n= 86)

Fig. 1. *Wnt1Cre;Brg1$^{f/f}$* embryos lack Brg1 in NCCs and NCC-derived tissues and die between E11.5 and E12.5. (*A–H*) Immunostaining of Brg1 (green) in neural crest, dorsal root ganglia, cardiac OFT, and forebrain of E10 *Wnt1Cre;Brg1$^{f/+}$* embryos (*A*, *C*, *E*, and *G*) and *Wnt1Cre;Brg1$^{f/f}$* embryos (*B*, *D*, *F*, and *H*). DAPI (DNA): blue. Dashed lines (*A* and *B*) denote the site of neural tube dorsal to which *Brg1* is deleted. *Brg1*-null NCCs that have reached the distal OFT are circled (*F*). (*I* and *J*) Gross morphology of control (*Wnt1Cre;Brg1$^{f/+}$*) and mutant (*Wnt1Cre;Brg1$^{f/f}$*) embryos at E10.5 (*I*) and E11.5 (*J*). (*K*) Frequency of live *Wnt1Cre;Brg1$^{f/f}$* embryos harvested at different embryonic dates.

ganglia, cardiac OFT, and forebrain vessels (Fig. 1 *A–H*). The *Wnt1Cre;Brg1$^{f/f}$* embryos developed grossly normally up to E11.5, when bleeding occurred in the forebrain but nowhere else in the body (Fig. 1 *I* and *J*); these embryos died between E11.5 and E12.5, with none surviving to E12.5 (Fig. 1*K*).

Brg1 Is Essential for Cerebral Vessel, PAA, and Cardiac OFT Development. To investigate the cause of embryonic lethality, we analyzed cerebral vessels, PAAs, and cardiac OFTs in *Wnt1Cre;Brg1$^{f/f}$* embryos. Bleeding consistently occurred bilaterally in the forebrain of *Wnt1Cre;Brg1$^{f/f}$* embryos at E11.5 (Fig. 1*J*). By Indian ink angiography (17), we observed that E10.5 *Wnt1Cre;Brg1$^{f/f}$* embryos displayed defects in PAAs, characterized by the near absence of PAA 3 and PAA 4 and enlargement of PAA 6 (Fig. 2 *A* and *B*). Through lineage tracing using *Wnt1Cre;R26R* mice (4, 16), we found that the cardiac OFTs of E10.5 *Wnt1Cre;Brg1$^{f/f}$* embryos was shortened by 41% ($P < 0.0001$), and the depth of NCC penetration into the heart was reduced by 52% ($P < 0.0001$) (Fig. 2 *C–F*). Thus, Brg1 functions in NCCs to regulate cerebral vessel function, PAA patterning, and OFT development. The massive forebrain bleeding will likely cause embryonic death.

Brg1 Inhibits Apoptosis and Promotes Proliferation and Differentiation of NCCs. To identify the cellular basis of these phenotypes, we tested the function of Brg1 in NCCs for cell apoptosis, proliferation, and differentiation. To test cell death, we examined E9 or E10 embryos by activated Caspase3 and TUNEL staining and found increased apoptosis in the neural crest and NCC-derived pharyngeal arch and dorsal root ganglia of *Wnt1Cre;Brg1$^{f/f}$* embryos (Fig. 3 *A* and *B* and Fig. S1 *A–F*). These findings suggest that Brg1 suppresses apoptosis of NCCs in vivo. For cell proliferation, we labeled E10 embryos with BrdU for 2 h and stained the embryos with BrdU antibody. The incorporation of BrdU in *Wnt1Cre;Brg1$^{f/f}$* NCCs was reduced by 45% ($P <$ 0.0001) (Fig. 3 *C–E*), indicating that Brg1 is essential for NCC proliferation in vivo.

To explore the cause of forebrain bleeding, we tested the differentiation of endothelium and SMCs of anterior cerebral vessels at E10.5. Immunostaining with endothelial and SMC markers identified normal endothelial marker Pecam1 and early SMC marker Vimentin in the cerebral vessels of E10.5 *Wnt1Cre;Brg1$^{f/f}$* embryos (Fig. S2 *A–D*). This finding suggests that endothelial differentiation and early differentiation of SMCs are normal in mutant embryos. However, the cerebral vascular SMCs of *Wnt1Cre;Brg1$^{f/f}$* embryos had severely diminished expression of smooth muscle myosin heavy chains (*Myh11*), a differentiation marker of mature SMCs (18) (Fig. 3 *F–H*). Because SMCs, but not endothelial cells, of forebrain vessels are derived from NCCs (6, 19), these results suggest that *Brg1*-null SMCs failed to mature to form a strong vessel wall. Such immature vascular wall may be fragile, leading to severe bleeding and embryonic lethality.

To further test the cell-autonomous role of Brg1 and develop cellular assays to study Brg1 biology in NCCs, we knocked down *Brg1* in Joma1.3 cells, a transformed murine NCC line that expresses early NCC markers and can be induced to differentiate into SMCs (20). We generated stable Joma1.3 NCCs by infecting these cells with lentivirus that allowed doxycycline (Dox)-inducible expression of shRNA against *Brg1* (designated siBrg1 NCCs), as well as a scrambled control shRNA (designated siCtrl NCCs) (Fig. 3 *I* and *J*). To test the efficiency of *Brg1* knockdown, we used quantitative RT-PCR (qRT-PCR) to quantitate *Brg1* mRNA in these stable NCCs. Within 48 h of Dox treatment, *Brg1* mRNA was knocked down by 58% in cultured NCCs (Fig. 3*K*), which was confirmed by Western blot analysis of Brg1 protein (Fig. 3*L*). This *Brg1* knockdown resulted in a 40% reduction ($P <$ 0.01) in the number of NCCs within 3 d of culture (Fig. 3*M*), suggesting that Brg1 triggers NCC death, inhibits NCC proliferation, or both. TUNEL staining revealed that *Brg1*

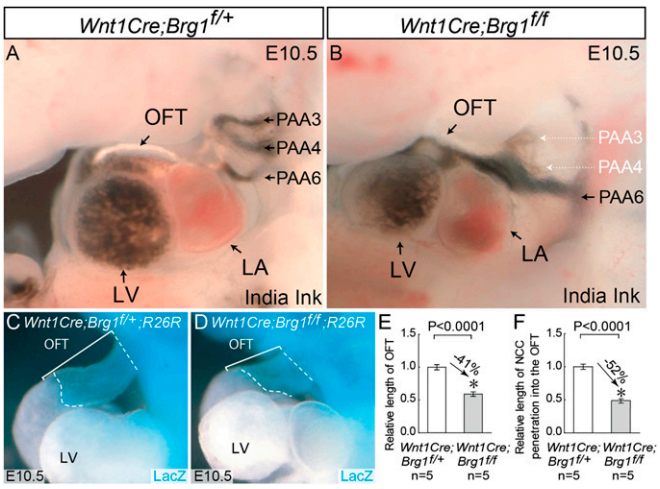

Fig. 2. Brg1 is essential for the development of PAAs and cardiac OFT. (*A* and *B*) India ink injection of the PAAs in *Wnt1Cre;Brg1$^{f/+}$* (*A*) and *Wnt1Cre;Brg1$^{f/f}$* E10.5 (*B*) embryos. The PAAs are numbered according to pharyngeal arch origin. (*C* and *D*) Whole-mount β-galactosidase staining (blue) of *Wnt1Cre;Brg1$^{f/+}$;R26R* (*C*) and *Wnt1Cre;Brg1$^{f/f}$;R26R* (*D*) embryos at E10.5. The bracketed regions indicate the length of cardiac OFT. The dashed lines denote the range of NCCs in the OFT. (*E* and *F*) Quantitation of the length of cardiac OFT (*E*; distance within the brackets) and NCC penetration into the OFT (*F*; distance between the dashed lines). The relative cardiac OFT length or NCC penetration into the OFT in *Wnt1Cre;Brg1$^{f/+}$* embryos at E10.5 is set at 1. Error bar indicates SEM. **P* statistically significant, Student *t* test. LV, left ventricle; LA, left atria.

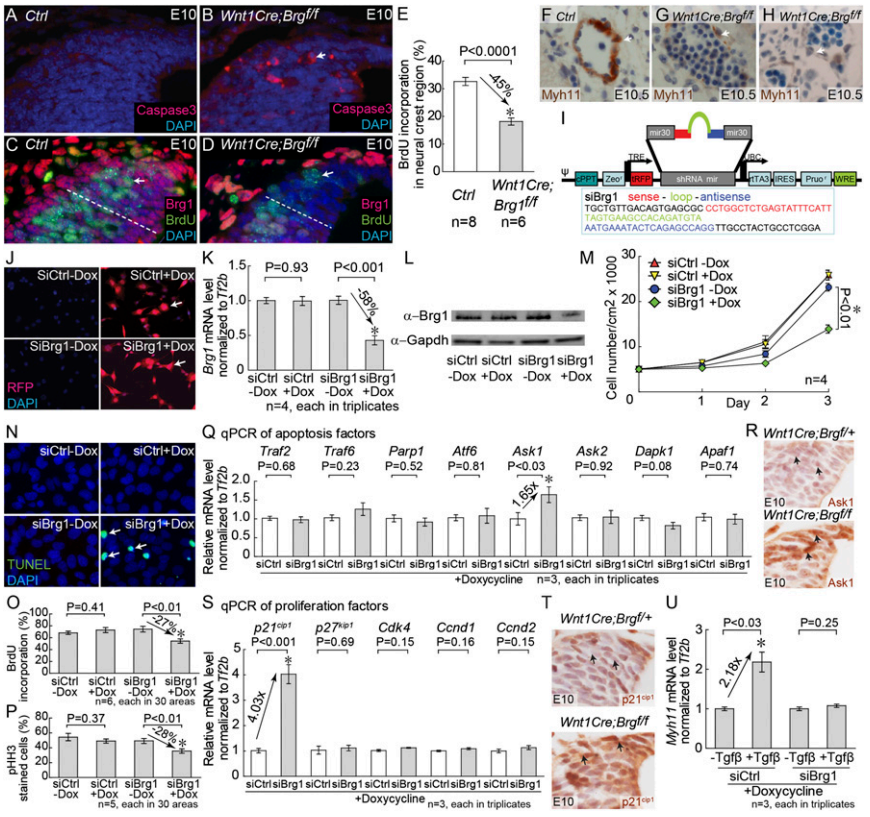

Fig. 3. Brg1 is essential for apoptosis inhibition, proliferation, and differentiation of NCCs. (*A* and *B*) Activated Caspase3 immunostaining (red) of control (*A*) and mutant (*Wnt1Cre;Brg1$^{f/f}$*) (*B*) embryos in the neural crest region at E10. DAPI (DNA), blue. (*C* and *D*) BrdU (green) and Brg1 (red) coimmunostaining of control (*C*) and mutant (*Wnt1Cre;Brg1$^{f/f}$*) (*D*) embryos in the neural crest region at E10. DAPI (DNA), blue. (*E*) Quantification of BrdU incorporation in the neural crest region of control and mutant (*Wnt1Cre; Brg1$^{f/f}$*) embryos at E10. (*F–H*) Myh11 immunostaining (brown) of control (*F*) and mutant (*Wnt1Cre; Brg1$^{f/f}$*) (*G* and *H*) embryos in the anterior cerebral arteries at E10.5. The counterstain was hematoxylin. (*I*) Schematic representation of the Dox-inducible lentiviral construct. The ubiquitin C (UBC) promoter drives the expression of reverse tetracycline transactivator 3 (rtTA3) along with the puromycin resistance gene used for selection of transduced cells. In the presence of Dox, rtTA3 binds to Tetracycline Response Elements (TRE) and activates the expression of a Turbo RFP and shRNAmir. The shRNAmir sequence used for mouse *Brg1* mRNA targeting is shown. (*J*) Dox-inducible expression of shRNAmir in Joma1.3 NCCs infected with Brg1 shRNA (siBrg1) or control shRNA (siCtrl) lentivirus that emits red fluorescence protein (RFP) in the presence of Dox. DAPI (DNA), blue. (*K* and *L*) shRNA-mediated down-regulation of Brg1 mRNA (*K*) and protein level (*L*). Brg1 mRNA or protein was examined by qRT-PCR or Western blot analysis of samples prepared from Brg1 and control shRNA-transduced Joma1.3 NCCs with or without Dox. (*M*) Quantification of Brg1 and control shRNA-transduced Joma1.3 NCCs with or without Dox. (*N*) TUNEL staining of Brg1 and control shRNA-transduced Joma1.3 NCCs with or without Dox. (*O* and *P*) Quantification of BrdU incorporation (*O*) and phosphohistone H3 (pHH3) immunostaining (*P*) of Brg1 and control shRNA-transduced Joma1.3 NCCs with or without Dox. (*Q*) Quantitation of apoptosis-related gene expression by qRT-PCR in Joma1.3 NCCs infected with lentivirus expressing control or anti-Brg1 shRNA. (*R*) Ask1 immunostaining (brown) of control (*Wnt1Cre;Brg1$^{f/+}$*) and mutant (*Wnt1Cre;Brg1$^{f/f}$*) embryos in the neural crest region at E10. The counterstain was hematoxylin. (*S*) Quantitation by qRT-PCR of genes regulating proliferation in Joma1.3 NCCs infected with lentivirus expressing control or anti-Brg1 shRNA. (*T*) p21^{cip1} immunostaining (brown) of control (*Wnt1Cre;Brg1$^{f/+}$*) and mutant (*Wnt1Cre;Brg1$^{f/f}$*) embryos in the neural crest region at E10. The counterstain was hematoxylin. (*U*) Quantitation of *Myh11* expression by qRT-PCR in Joma1.3 NCCs infected with lentivirus expressing control or anti-Brg1 shRNA with or without Tgfβ. Error bar indicates SEM. **P* statistically significant, Student *t* test.

knockdown led to apoptosis of NCCs (Fig. 3*N*), whereas BrdU incorporation and phosphohistone H3 (pHH3) staining were associayed with 27% and 28% decreases in proliferation, respectively, with *Brg1* knockdown (Fig. 3 *O* and *P*). These findings indicate that the decrease in siBrg1 NCCs is caused by a combination of increased cell apoptosis and decreased cell proliferation, consistent with the in vivo observations.

We then used qRT-PCR to identify factors contributing to the apoptosis of *Brg1*-deficient NCCs. We tested the expression of apoptosis-regulating genes *Traf2*, *Traf6*, *Parp1*, *Atf6, Ask1*, *Ask2*, *Dapk1*, and *Apaf1* in siBrg1 NCCs (21–28). Of these genes, only *Ask1* (*apoptosis signal-regulating kinase 1*) exhibited increased expression (a 1.65-fold increase; $P < 0.03$) in siBrg1NCCs; the other genes showed no significant changes (Fig. 3*Q*). We then tested the in vivo role of Ask1 by immunostaining. Ask1 proteins were minimal or absent in the control but were abundant in *Wnt1Cre;Brg1$^{f/f}$* NCCs (Fig. 3*R*). Given that Ask1 activates caspase to execute apoptosis (24), and that both Ask1 and Caspase3 were activated in *Brg1*-null NCCs (Fig. 3 *B* and *R*), our in vitro and in vivo findings suggest that Brg1 suppresses Ask1 in NCCs to prevent Ask1 from activating caspase to cause cell apoptosis.

We also used qRT-PCR to identify factors contributing to NCC proliferation. We examined siBrg1 NCCs for the expression of cell cycle-regulating genes *p21^{cip1}*, *p27^{kip1}*, *Cdk4*, *Cyclin D1* (*Ccnd1*), and *Cyclin D2* (*Ccnd2*) (29, 30). Of these genes, only *p21^{cip1}* (*Cdkn1a*), which inhibits cyclin E-Cdk2 and cyclin D-Cdk4/6 (29), showed a significant increase (4.03-fold; $P < 0.001$) in siBrg1 NCCs; the other genes exhibited no significant changes (Fig. 3*S*). To test whether p21^{cip1} was up-regulated in vivo, we immunostained p21^{cip1} in the NCCs of *Wnt1Cre;Brg1$^{f/f}$* mice. Immunostaining indeed showed an increase of p21^{cip1} in *Brg1*-null NCCs (Fig. 3*T*). Given that p21^{cip1} is a cell cycle inhibitor, these findings suggest that Brg1 suppresses p21^{cip1} in NCCs to promote cell proliferation in vivo. The suppression of Ask1 and p21^{cip1} by Brg1 provides a mechanism by which Brg1 inhibits apoptosis and maintains proliferation of NCCs in vivo.

To test the effect of Brg1 on the differentiation of NCCs into SMCs, we treated siBrg1 NCCs with Tgfβ to induce their differentiation into mature SMCs expressing *Myh11* (20). qRT-PCR showed that Tgfβ induced *Myh11* expression in siCtrl NCs, but not in siBrg1 NCCs (Fig. 3*U*), suggesting that Brg1 is necessary for the differentiation of NCCs into mature SMCs, consistent with in vivo observations (Fig. 3*G*). Collectively, both the in vivo and culture studies indicate that Brg1 functions in a cell-autonomous manner through distinct pathways to regulate the survival, proliferation, and differentiation of NCCs.

Brg1 Is Essential for *PlexinA2* Activation and NCC Migration. By Brg1 immunostaining and lineage tracing of NCCs, we observed a 44% reduction of NCCs in the cardiac OFT (Fig. S3) and a failure of *Brg1*-null NCCs to migrate deeply into the proximal OFT (Fig. 2 *C–F*). We hypothesized the presence of additional migratory defects in *Brg1*-null NCCs. Because Alk2/Tgfβ and PlexinA2 are essential for NCC migration44 into the OFT (31–33), we tested whether expression of these genes was changed in *Wnt1Cre;Brg1$^{f/f}$* embryos. RNA in situ hybridization showed that

Alk2 and *Tgfβ2* were normally expressed in the OFT (Fig. S4 *A*–*D*). In contrast, *PlexinA2* was severely reduced in *Brg1*-null NCCs at the neural crest of rhombomere 6–8 and in the OFT of *Wnt1Cre;Brg1$^{f/f}$* embryos (Fig. 4 *A*–*D*). These observations indicate that Brg1 is essential for *PlexinA2* expression in NCCs, consistent with the failed migration of *Brg1*-null NCCs into the proximal OFT.

To test if Brg1 was essential for NCC movement in culture, we first examined siBrg1 NCCs for *PlexinA2* expression. qRT-PCR showed that *Brg1* knockdown reduced *PlexinA2* by 29% ($P < 0.02$) without changes of other migratory factors such as *PlexinD1* and *Nrp1* (33) (Fig. 4*E*). Next, we used microscopy to live image and measure the migratory speed of Joma1.3 NCC in response to the chemokine Sema3C, which promotes NCCs migration into cardiac OFT (34). We found that Sema3c proteins increased the speed of Joma1.3 cell migration by 4.14 folds; however, with *Brg1* knockdown, Sema3c increased the migratory speed by only 1.36 folds (Fig. 4*F*). Therefore, Brg1 knockdown reduced the cell migration by 67% (from 4.14- to 1.36-fold; $P < 0.001$). The requirement of Brg1 for the migratory response of NCCs to Sema3C is consistent with the reduction of *PlexinA2* in *Brg1*-deficient NCCs. Collectively, the reduced penetration of *Brg1*-null NCCs into the OFT and the reduction of *PlexinA2* in *Brg1*-null NCCs, as well as the reduced movement of *Brg1*-deficient NCCs support that Brg1 is required for migration of NCCs into the proximal OFT in vivo.

***PlexinA2* Is a Direct Target of Brg1.** To test if Brg1 directly activated *PlexinA2,* we used ChIP and quantitative PCR (qPCR) to examine the binding of Brg1 to *PlexinA2* promoter. With sequence alignment (www.dcode.org), we identified nine regions (p1–p9) in the proximal 9.5-kb promoter of mouse *PlexinA2* that are evolutionarily conserved among mouse, dog, monkey, rat, or human (Fig. 4*G*). After validating Brg1, Chd7, and *PlexinA2* expression in the neural crest (Figs. 1A and 4A and Fig. S5*A*), we dissected neural crest tissues from rhombomere 6–8 region of E9 embryos as indicated (Fig. 4*H*). ChIP-qPCR analyses of cardiac neural crest tissues (~25–30 embryos per ChIP reation) using anti-Brg1 antibody (35, 36) showed that Brg1 was highly enriched within the conserved p1–p9 regions, but not in the nonconserved region of *PlexinA2* (Fig. 4 *I* and *J*). In Joma1.3 NCCs that also had Brg1, Chd7, and PlexinA2 (Fig. S5 *B* and *C*), ChIP analysis

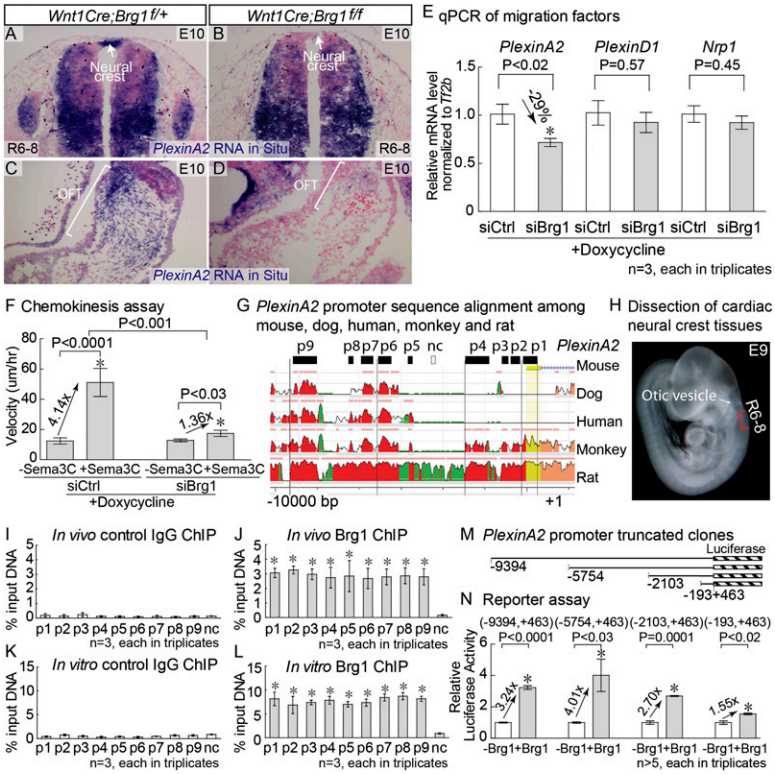

Fig. 4. Brg1 is essential for *PlexinA2* activation and NCC migration. (*A* and *B*) RNA in situ hybridization of *PlexinA2* (blue) in the neural crest region (rhombomere 6–8 level) of control (*Wnt1Cre;Brg1$^{f/+}$*) (*A*) and mutant (*Wnt1Cre;Brg1$^{f/f}$*) (*B*) embryos at E10. The counterstain was nuclear fast red. R, rhombomere. (*C* and *D*) RNA in situ hybridization of *PlexinA2* (blue) in the OFT of control (*Wnt1Cre;Brg1$^{f/+}$*) (*C*) and mutant (*Wnt1Cre;Brg1$^{f/f}$*) (*D*) embryos at E10. The counterstain was nuclear fast red. (*E*) Quantitation of genes regulating cell migration by qRT-PCR in Joma1.3 NCCs infected with lentivirus expressing control or anti-Brg1 shRNA. Error bar indicates SEM. **P* statistically significant, Student *t* test. (*F*) Quantification of cell chemokinetic velocity of Dox-treated Brg1 and control shRNA-transduced Joma1.3 NCCs in the presence or absence of Sema3C. Error bar indicates SEM. **P* statistically significant, Student *t* test. (*G*) Sequence alignment of the *PlexinA2* locus from mouse, dog, human, monkey, and rat. Peak heights reflect the degree of sequence homology. Evolutionarily conserved regions (black boxes, p1–p9) and the nonconserved (nc) region (white box) were further analyzed by ChIP. The DNA positions are relative to the transcriptional start site (+1). Red indicates promoter elements; salmon, introns; yellow, untranslated regions; green, transposons and simple repeats. (*H*) Indication of dissected region from E9 embryos for ChIP and co-IP assays. R, rhombomere. (*I* and *J*) qPCR quantification of control IgG (*I*) and Brg1 (*J*) antibody-immunoprecipitated chromatin from E9 cardiac neural crest tissues using primers targeting *PlexinA2* promoter (p1–p9 and nc). Signals were standardized to the percentage of input DNA. **P* < 0.05, statistically significant from respective IgG controls (Fig. 4*I*). (*K* and *L*) qPCR quantification of control IgG (*K*) and Brg1 (*L*) antibody-immunoprecipitated chromatin from Joma1.3 NCCs using primers targeting *PlexinA2* promoter (p1–p9 and nc). Signals were standardized to the percentage of input DNA. **P* < 0.05, statistically significant from respective IgG controls (Fig. 4*K*). (*M* and *N*) Episome-based reporter assays using the indicated *PlexinA2* promoter regions cloned in luciferase expression plasmids (*M*), with luciferase activity normalized to a cotransfected *Renilla* luciferase control (*N*). Error bar indicates SEM. **P* statistically significant, Student *t* test.

demonstrated similar Brg1 enrichment within the *PlexinA2* p1–p9, but not within nonconserved regions (Fig. 4 *K* and *L*). No Brg1 enrichment was detected on the negative control *β-MHC* (35) (Fig. S6). Therefore, in NCCs, Brg1 proteins are present on the conserved regions of proximal *PlexinA2* promoter.

To study the activity of Brg1 on the *PlexinA2* promoter, we cloned the full-length proximal *PlexinA2* promoter (−9394, +463) and truncated *PlexinA2* promoters (−5754, +463), (−2103, +463), and (−193, +463) into an episomal luciferase reporter pREP4 (Fig. 4*M*). The pREP4 plasmid is an Epstein–Barr virus-based episomal vector that undergoes chromatinization after transfection into mammalian cells (37) and thus is suitable for studying the chromatin and transcription activity of Brg1 on gene promoters (35–37). Given the resistance of Joma1.3 NCCs to transfection, the *PlexinA2* reporter plasmids and Brg1-expressing plasmids (35) were cotransfected into 293T cells as a surrogate for reporter assays. Measuring the luciferase activity driven by *PlexinA2* reporter revealed that Brg1 activated the *PlexinA2* full-length promoter activity by 3.24-fold. Deletional analysis (35) of *PlexinA2* promoter showed a length-dependent induction of promoter activities by Brg1, with 4.01-fold for the (−5754, +463) promoter, 2.70-fold for the (−2103, +463) promoter, and 1.55-fold for the (−193, +463) promoter (Fig. 4*N*), suggesting Brg1 activity on multiple binding sites (p1–p9). These results, together with ChIP analysis results, indicate direct transcriptional activation of *PlexinA2* by Brg1.

Brg1 Cooperates with Chd7 to Activate *PlexinA2*. Because Chd7 mutations causes CHARGE syndrome with PAA and OFT defects (13), we asked whether Brg1 cooperated with Chd7 to regulate NCC development. We first investigated the direct binding of Chd7 and Brg1 on the *PlexinA2* promoter. Interestingly, ChIP analysis of cardiac neural crest tissue (Fig. 5*A*) and Joma1.3 NCCs (Fig. 5*B*) using anti-Chd7 antibody showed that Chd7, like Brg1, was highly enriched within the conserved p1–p9 regions of *PlexinA2* promoter, but not in the nonconserved region and not in the negative control *β-MHC* promoter (Fig. S6). This Chd7 ChIP pattern suggests that Brg1 and Chd7 are in close proximity on the *PlexinA2* promoter. To further test the physical interaction of Brg1 and Chd7, we performed coimmunoprecipitation (co-IP) using cardiac neural crest tissues (~10–15 E9 embryos for each reaction) and found that Chd7 formed complexes with Brg1 in the neural crest (Fig. 5*C*).

To test Brg1–Chd7 transcriptional interaction on *PlexinA2*, we overexpressed Brg1, Chd7, or both in different amounts in 293T cells and performed reporter analysis of the *PlexinA2* promoter. *PlexinA2* promoter activity was activated in a dose-dependent manner by Brg1 and by Chd7 (Fig. 5*D*), and coexpression of Brg1 and Chd7 had roughly twofold synergetic effects on promoter activation (Fig. 5*D*). Collectively, the results of our ChIP, co-IP, and reporter assays indicate the presence of Brg1–Chd7 complex on the *PlexinA2* promoter to activate *PlexinA2*, essential for navigation of NCCs into proximal OFT.

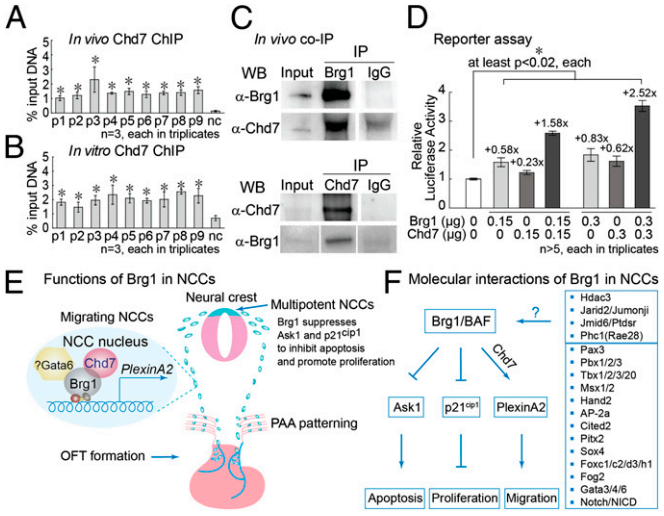

Fig. 5. Brg1 cooperates with Chd7 to activate *PlexinA2*. (*A*) qPCR quantification of Chd7 antibody-immunoprecipitated chromatin from E9 cardiac neural crest tissues using primers targeting *PlexinA2* promoter [p1–p9 and nonconserved (nc)]. Signals were standardized to the percentage of input DNA. **P* < 0.05, statistically significant from respective IgG controls (Fig. 4*I*). (*B*) qPCR quantification of Chd7 antibody-immunoprecipitated chromatin from Joma1.3 NCCs using primers targeting *PlexinA2* promoter (p1–p9 and nc). Signals were standardized to the percentage of input DNA. **P* < 0.05, statistically significant from respective IgG controls (Fig. 4*K*). (*C*) Coimmunoprecipitation of Brg1 and Chd7 in E9 cardiac neural crest tissues. (*D*) Luciferase reporter assays of *PlexinA2* promoter (−9394, +463) in 293T cells cotransfected with Brg1 and/or Chd7 at indicated amounts. Error bar indicates SEM. **P* statistically significant, Student *t* test. (*E*) Functions of Brg1 in NCC survival, migration, and differentiation. (*F*) Model of molecular interactions of Brg1 in NCCs. Brg1 partners with Chd7, histone modifiers, and transcription factors to program gene expression in NCCs.

Discussion

Our findings demonstrate a unique role of Brg1 and its downstream pathways for NCC survival, differentiation, and migration (Fig. 5 *E* and *F*). Brg1 inhibits NCC apoptosis at least in part by suppressing Ask1, an apoptosis-signal regulating kinase that activates the caspase pathway to trigger cell apoptosis (24). In parallel, Brg1 promotes NCC proliferation partly through its suppression of $p21^{cip}$, a cell cycle inhibitor (29). Brg1 also promotes the differentiation of NCCs into mature vascular SMCs. *Brg1*-null NCCs are unable to differentiate into Myh11-expressing SMCs, resulting in weakened vessel walls, massive bleeding, and embryonic death. In addition, Brg1 in NCCs is required for PAA patterning. The near absence of PAA 3 and 4 arteries, which are precursors of common carotid arteries and aortic arch, suggests that aberrant great arteries would develop in NCC *Brg1*-null embryos if these embryos could survive the bleeding. Finally, Brg1 is essential for navigating NCCs to the heart for OFT development. *Brg1*-deficient NCCs fail to express *PlexinA2*, which encodes a coreceptor for semaphorin signaling molecules to guide NCCs into the proximal OFT (32–34). The vital role of Brg1 in multiple NCC functions indicates that active chromatin restructuring is essential for NCCs to execute their various developmental tasks.

Gene programing in NCCs at the chromatin level is largely unknown (8–10). Hdac3 in NCCs is required to regulate PAA and OFT development; however, its direct target genes are unknown (38). Some histone-modifying enzymes are also known to regulate OFT development, but their cellular sites of actions are undefined. Germ line deletion of *Jarid2*/*Jumonji* or *Jmid6*/*Ptdsr* causes double-outlet right ventricle (39, 40), whereas the disruption of *Phc1* (*Rae28*), encoding a member of the polycomb repressive complex 1, results in tetralogy of Fallot and double-outlet right ventricle (41). Tissue-specific disruption of these histone modifiers in NCCs will be necessary to test their cell-autonomous roles in NCCs for heart development. Brg1 is the sole ATP-dependent chromatin-remodeling factor known to have an intrinsic role in NCCs for mammalian heart development. Assembly of the Brg1–Chd7 complex on the chromatin of *PlexinA2* promoter to activate *PlexinA2* and navigate NCCs suggests that Chd7 also has a cell-autonomous role in NCCs for PAA/OFT development. Tissue-specific gene deletion of Chd7 in mice will be essential to precisely define the action site(s) of Chd7 for heart development. Further studies of the interactions among Brg1, Chd7, Hdac3, and other histone modifiers will provide a deeper understanding of how the epigenome of NCCs is

dynamically programmed for to perform a multitude of developmental functions.

Chromatin regulators interact with transcription factors to control gene expression. Gata6, a transcription factor with mutations identified in patients with OFT defects, is essential for the activation of *PlexinA2* in NCCs (42, 43). Other transcription factors, such as Pax3 and Pbx1, are required to program NCCs for PAA/OFT development (16, 44–46). Determining how the Brg1–Chd7 complex interacts with these transcription factors will be crucial to elucidating the gene programming mechanism in NCCs for cardiovascular development.

Our findings provide direct evidence in mammalian heart development to strengthen the mechanistic links among Brg1, Chd7, NCC, and CHARGE syndrome. However, many cells besides NCCs are required for cardiac OFT development, including second heart field progenitor cells, endocardial cells, and myocardial cells (8). Further investigation of whether Brg1 interacts with Chd7 in those non-NCC tissues for heart development will provide a better understanding of the interactions of chromatin remodelers relevant to CHARGE syndrome. These studies will also elucidate how those cells are programmed by chromatin remodelers to non–cell-autonomously influence NCC survival, differentiation, or migration during embryonic development.

Materials and Methods

Immunostaining, RNA in situ hybridization, qRT-PCR, ChIP, and reporter assays have been described previously (47), as have *Brg1$^{f/f}$* (15), *Wnt1Cre* (16), and *R26R* (48) mice. The date on which a vaginal plug was observed in the mice was set as E0.5. Animal care and handling were in accordance with the regulations of Administrative Panel for Laboratory Animal Care at Stanford University and guidelines of the National Institutes of Health. Detailed information on materials and experimental procedures is provided in *SI Materials and Methods*.

ACKNOWLEDGMENTS. We thank Dr. P. Chambon for providing the *Brg1$^{f/f}$* mice. C.-P.C. was supported by the March of Dimes Foundation, the CHARGE Syndrome Foundation, an American Heart Association Established Investigator Award, the National Institutes of Health (NIH), and the California Institute of Regenerative Medicine. W.L. and Y.X. were supported by the Oak Foundation and Stanford Child Health Research Institute. Y.X. was also supported by the American Heart Association and C.S. by an NIH fellowship and the March of Dimes Foundation.

1. Gilbert SF (2010) *Developmental Biology* (Sinauer Associates, Sunderland, MA), 9th Ed, pp xxi, 711, 780.
2. Kirby ML (2007) *Cardiac Development* (Oxford University Press, London), p 3500.
3. Kirby ML, Gale TF, Stewart DE (1983) Neural crest cells contribute to normal aorticopulmonary septation. *Science* 220(4601):1059–1061.
4. Jiang X, Rowitch DH, Soriano P, McMahon AP, Sucov HM (2000) Fate of the mammalian cardiac neural crest. *Development* 127(8):1607–1616.
5. Li J, Chen F, Epstein JA (2000) Neural crest expression of Cre recombinase directed by the proximal Pax3 promoter in transgenic mice. *Genesis* 26(2):162–164.
6. Etchevers HC, Vincent C, Le Douarin NM, Couly GF (2001) The cephalic neural crest provides pericytes and smooth muscle cells to all blood vessels of the face and forebrain. *Development* 128(7):1059–1068.
7. Hutson MR, Kirby ML (2003) Neural crest and cardiovascular development: A 20-year perspective. *Birth Defects Res C Embryo Today* 69(1):2–13.
8. Lin CJ, Lin CY, Chen CH, Zhou B, Chang CP (2012) Partitioning the heart: Mechanisms of cardiac septation and valve development. *Development* 139(18):3277–3299.
9. Chang CP, Bruneau B (2012) Epigenetics and cardiovascular development. *Annu Rev Physiol* 74:41–68.
10. Han P, Hang CT, Yang J, Chang CP (2011) Chromatin remodeling in cardiovascular development and physiology. *Circ Res* 108(3):378–396.
11. Ho L, Crabtree GR (2010) Chromatin remodelling during development. *Nature* 463 (7280):474–484.
12. Bajpai R, et al. (2010) CHD7 cooperates with PBAF to control multipotent neural crest formation. *Nature* 463(7283):958–962.
13. Vissers LE, et al. (2004) Mutations in a new member of the chromodomain gene family cause CHARGE syndrome. *Nat Genet* 36(9):955–957.
14. Zentner GE, Layman WS, Martin DM, Scacheri PC (2010) Molecular and phenotypic aspects of CHD7 mutation in CHARGE syndrome. *Am J Med Genet A* 152A(3):674–686.
15. Sumi-Ichinose C, Ichinose H, Metzger D, Chambon P (1997) SNF2beta-BRG1 is essential for the viability of F9 murine embryonal carcinoma cells. *Mol Cell Biol* 17(10):5976–5986.
16. Chang CP, et al. (2008) Pbx1 functions in distinct regulatory networks to pattern the great arteries and cardiac outflow tract. *Development* 135(21):3577–3586.
17. Chang CP (2012) Analysis of the patterning of cardiac outflow tract and great arteries with angiography and vascular casting. *Methods Mol Biol* 843:21–28.
18. Aikawa M, et al. (1998) Lipid lowering promotes accumulation of mature smooth muscle cells expressing smooth muscle myosin heavy chain isoforms in rabbit atheroma. *Circ Res* 83(10):1015–1026.
19. Bergwerff M, Verberne ME, DeRuiter MC, Poelmann RE, Gittenberger-de Groot AC (1998) Neural crest cell contribution to the developing circulatory system: Implications for vascular morphology? *Circ Res* 82(2):221–231.
20. Maurer J, et al. (2007) Establishment and controlled differentiation of neural crest stem cell lines using conditional transgenesis. *Differentiation* 75(7):580–591.
21. Jing G, Wang JJ, Zhang SX (2012) ER stress and apoptosis: A new mechanism for retinal cell death. *Exp Diabetes Res* 2012:589589.
22. Bharti AC, Aggarwal BB (2004) Ranking the role of RANK ligand in apoptosis. *Apoptosis* 9(6):677–690.
23. Yu SW, et al. (2002) Mediation of poly(ADP-ribose) polymerase-1-dependent cell death by apoptosis-inducing factor. *Science* 297(5579):259–263.
24. Hatai T, et al. (2000) Execution of apoptosis signal-regulating kinase 1 (ASK1)-induced apoptosis by the mitochondria-dependent caspase activation. *J Biol Chem* 275(34): 26576–26581.
25. Fujisawa T, Takeda K, Ichijo H (2007) ASK family proteins in stress response and disease. *Mol Biotechnol* 37(1):13–18.
26. Yoo HJ, et al. (2012) DAPk1 inhibits NF-κB activation through TNF-α and INF-γ-induced apoptosis. *Cell Signal* 24(7):1471–1477.
27. Degterev A, Yuan J (2008) Expansion and evolution of cell death programmes. *Nat Rev Mol Cell Biol* 9(5):378–390.
28. Kung G, Konstantinidis K, Kitsis RN (2011) Programmed necrosis, not apoptosis, in the heart. *Circ Res* 108(8):1017–1036.
29. Harper JW, Adami GR, Wei N, Keyomarsi K, Elledge SJ (1993) The p21 Cdk-interacting protein Cip1 is a potent inhibitor of G1 cyclin-dependent kinases. *Cell* 75(4):805–816.
30. Sridhar J, Akula N, Pattabiraman N (2006) Selectivity and potency of cyclin-dependent kinase inhibitors. *AAPS J* 8(1):E204–E221.
31. Kaartinen V, et al. (2004) Cardiac outflow tract defects in mice lacking ALK2 in neural crest cells. *Development* 131(14):3481–3490.
32. Brown CB, et al. (2001) PlexinA2 and semaphorin signaling during cardiac neural crest development. *Development* 128(16):3071–3080.
33. Toyofuku T, et al. (2008) Repulsive and attractive semaphorins cooperate to direct the navigation of cardiac neural crest cells. *Dev Biol* 321(1):251–262.
34. Feiner L, et al. (2001) Targeted disruption of semaphorin 3C leads to persistent truncus arteriosus and aortic arch interruption. *Development* 128(16):3061–3070.
35. Hang CT, et al. (2010) Chromatin regulation by Brg1 underlies heart muscle development and disease. *Nature* 466(7302):62–67.
36. Stankunas K, et al. (2008) Endocardial Brg1 represses ADAMTS1 to maintain the microenvironment for myocardial morphogenesis. *Dev Cell* 14(2):298–311.
37. Liu R, et al. (2001) Regulation of CSF1 promoter by the SWI/SNF-like BAF complex. *Cell* 106(3):309–318.
38. Singh N, et al. (2011) Histone deacetylase 3 regulates smooth muscle differentiation in neural crest cells and development of the cardiac outflow tract. *Circ Res* 109(11): 1240–1249.
39. Lee Y, et al. (2000) Jumonji, a nuclear protein that is necessary for normal heart development. *Circ Res* 86(9):932–938.
40. Schneider JE, et al. (2004) Identification of cardiac malformations in mice lacking Ptdsr using a novel high-throughput magnetic resonance imaging technique. *BMC Dev Biol* 4:16.
41. Takihara Y, et al. (1997) Targeted disruption of the mouse homologue of the *Drosophila* polyhomeotic gene leads to altered anteroposterior patterning and neural crest defects. *Development* 124(19):3673–3682.
42. Kodo K, et al. (2009) GATA6 mutations cause human cardiac outflow tract defects by disrupting semaphorin-plexin signaling. *Proc Natl Acad Sci USA* 106(33):13933–13938.
43. Lepore JJ, et al. (2006) GATA-6 regulates semaphorin 3C and is required in cardiac neural crest for cardiovascular morphogenesis. *J Clin Invest* 116(4):929–939.
44. Stankunas K, et al. (2008) Pbx/Meis deficiencies demonstrate multigenetic origins of congenital heart disease. *Circ Res* 103(7):702–709.
45. Epstein J (1996) Pax3, neural crest and cardiovascular development. *Trends Cardiovasc Med* 6(8):255–260.
46. Olaopa M, et al. (2011) Pax3 is essential for normal cardiac neural crest morphogenesis but is not required during migration nor outflow tract septation. *Dev Biol* 356(2):308–322.
47. Chang CP, et al. (2004) A field of myocardial-endocardial NFAT signaling underlies heart valve morphogenesis. *Cell* 118(5):649–663.
48. Soriano P (1999) Generalized lacZ expression with the ROSA26 Cre reporter strain. *Nat Genet* 21(1):70–71.